2015 International Symposium on Nonlinear Theory and its Applications
NOLTA2015, Kowloon, Hong Kong, China, December 1-4, 2015

Localization of eigenvectors in advection networks

Shigefumi Hata

Department of Mathematical Science and Advanced Technology,
Japan Agency for Marine-Earth Science and Technology (JAMSTEC)
3173-25, Showa-machi, Kanazawa-ku, Yokohama-city, Kanagawa, 236-0001, Japan
Email: shata@jamstec.go.jp

Abstract—Advection is a general transport mechanism whereby substances are conveyed by bulk flows. In network-organized systems, advective processes are described by using the advection matrix. Eigenvectors of the advection matrix tend to localize on a subset of network nodes which have similar flow intensities. Although this localization property can be observed numerically in a wide range of networks, no theoretical explanation has been proposed. In this paper, we establish a theoretical approach to explain the localization property on the basis of the perturbation approximation of the advection matrix. We demonstrate the ability of the proposed theory to predict the localizing pattern of eigenvectors for several classes of random networks.

1. Introduction

Advection is a general transport mechanism whereby substances are passively conveyed by bulk flows. Advective processes are ubiquitously found in nature and have been extensively studied in a wide range of research fields [1, 2, 3]. One of the central topics of this field of research is the collective dynamics of particles advected by turbulent flows. The statistical properties of the advection of passive particles have also attracted much attention.

Advective dynamics have mainly been studied for continuous media; however, they can also be considered in network-organized systems. In an advection network, substances occupy each node and are transported by flows along connecting links. Such a system may arise when we consider a network of pipelines through which bulk flows convey oil or pollutant to distribution branches or final destinations. Another such example would be a transportation network, in which traffic flows are established by trains, ships, or aircraft on regularly scheduled services between rail stations, ocean harbors, or airports. To describe the transport dynamics in these systems, we recently proposed a mathematical formulation of the advection equation in network-organized systems [4].

In the network advection equation, the time evolution of the concentration of particles at each node is described by the advection matrix, which has the remarkable property of having its eigenvectors localized on a subset of network nodes. Namely, each eigenvector tends to have relatively large values on the subset. This localization property plays a decisive role in mixing dynamics of passive particles. In advection networks, particle concentrations always equilibrate to a uniform distribution. The equilibration firstly occurs in the subset of nodes through which strong flows are passing and, gradually spreads to the entire network. Such dynamics can be explained by means of the localizing advection eigenvectors [4].

Although the localization property can be observed in a wide range of networks, the property has only been shown to exist numerically. Thus, no theoretical evidence of its presence has been so far proposed. In this paper, we provide a theoretical explanation of the localization property of the advection eigenvectors. Based on perturbation theory, a standard approximation technique in quantum mechanics, the localization of eigenvectors is qualitatively predicted. We apply the developed theory to several classes of advection networks for illustration.

2. Localization of advection eigenvectors

2.1. Advection matrix

Let us briefly review the derivation of the advection matrix. We consider a network of size N, which is formed by discrete nodes labeled by $i = 1, 2, \cdots, N$ and connected by directed links. Flows are passing over the links to convey substances. The network architecture is determined by the adjacency matrix $\mathbf{A} = \{A_{ij}\}$ of which the value of the element is $A_{ij} = 1$, if there is a link from node j to node i; otherwise its value is $A_{ij} = 0$. We consider that no self-loops exist in the network so that $A_{ii} = 0$ holds for any i. The transportation capacity of each link is specified by the weight matrix $\mathbf{W} = \{W_{ij}\}$.

We employ a stochastic description for advective transport in the network. If a node has multiple outgoing links, a single particle on the node will be transported over one of them with a certain probability. Stochastic transport of this nature in network-organized systems can be described as a Markov process, in which the time evolution of the concentrations θ_i of the particles at node i is given by

$$\frac{\partial \theta_i}{\partial t} = \sum_{j=1}^{N} \left(\nu_{ij} A_{ij} \theta_j - \nu_{ji} A_{ji} \theta_i \right), \tag{1}$$

where ν_{ij} is the transition probability of a single particle from node j to node i. We assume that ν_{ij} is proportional

to the intensity J_{ij} of the flow along the respective link, $v_{ij} = \nu J_{ij}$, where ν is a normalization constant. It is also assumed that the flows are incompressible such that the total incoming flow is equal to the total outgoing flow in each node. Thus, the condition

$$X_i = \sum_{j=1}^{N} J_{ij}A_{ij} = \sum_{j=1}^{N} J_{ji}A_{ji}, \tag{2}$$

should hold at any node i, where we introduce the variable X_i representing the total passing flow in node i for convenience. The flow X_i is divided among the outgoing links according to their relative transportation capacities W_{ij}, so that we have

$$J_{ji} = \frac{W_{ji}A_{ji}}{\sum_{l=1}^{N} W_{li}A_{li}} X_i. \tag{3}$$

We consider only those networks in which each node has at least one outgoing connection such that $\sum_{l=1}^{N} W_{li}A_{li} \neq 0$ and J_{ji} does not diverge. By substituting the expression (3) into Eq. (2), we have equations

$$\sum_{j=1}^{N} \left(\frac{W_{ij}A_{ij}}{\sum_{l=1}^{N} W_{lj}A_{lj}} - \delta_{ij} \right) X_j = 0, \tag{4}$$

of which the flows X_i at each node can be found as solutions. We normalize $\{X_i\}$ so that the total flow in the network is fixed at $\sum_{i=1}^{N} X_i = 1$. For convenience, the node indices $\{i\}$ are enumerated according to the flows X_i, so that

$$X_1 \geq X_2 \geq \cdots \geq X_N, \tag{5}$$

holds. Once the total passing flows X_i on the nodes are determined, the flow intensities J_{ij} for the links can be obtained by using Eq. (3).

The advection matrix $\{M_{ij}\}$ is defined by $M_{ij} = J_{ij}A_{ij} - \sum_{l=1}^{N} J_{li}A_{li}\delta_{ij}$, such that the time evolution in Eq. (1) can be rewritten as

$$\dot{\theta}_i = \nu \sum_{j=1}^{N} M_{ij}\theta_j. \tag{6}$$

By rescaling the time as $\nu t \to t$, we can set $\nu = 1$ without loss of generality.

2.2. Advection eigenvectors

The advection eigenvector $\vec{\psi}^{(\alpha)}$ and the corresponding eigenvalue $\Lambda^{(\alpha)}$ are defined by the equation

$$\sum_{j=1}^{N} M_{ij}\psi_j^{(\alpha)} = \Lambda^{(\alpha)}\psi_i^{(\alpha)}, \tag{7}$$

for $\alpha = 1, \cdots, N$. It can easily be checked that the advection matrix is negative semidefinite and, therefore, the real parts of all eigenvalues are nonpositive, $\mathrm{Re}\Lambda^{(\alpha)} \leq 0$. For convenience, the eigenmode index α is sorted in increasing order of the real part of the eigenvalues such that we have inequalities

$$\mathrm{Re}\Lambda^{(1)} \leq \mathrm{Re}\Lambda^{(2)} \leq \cdots \leq \mathrm{Re}\Lambda^{(N)}. \tag{8}$$

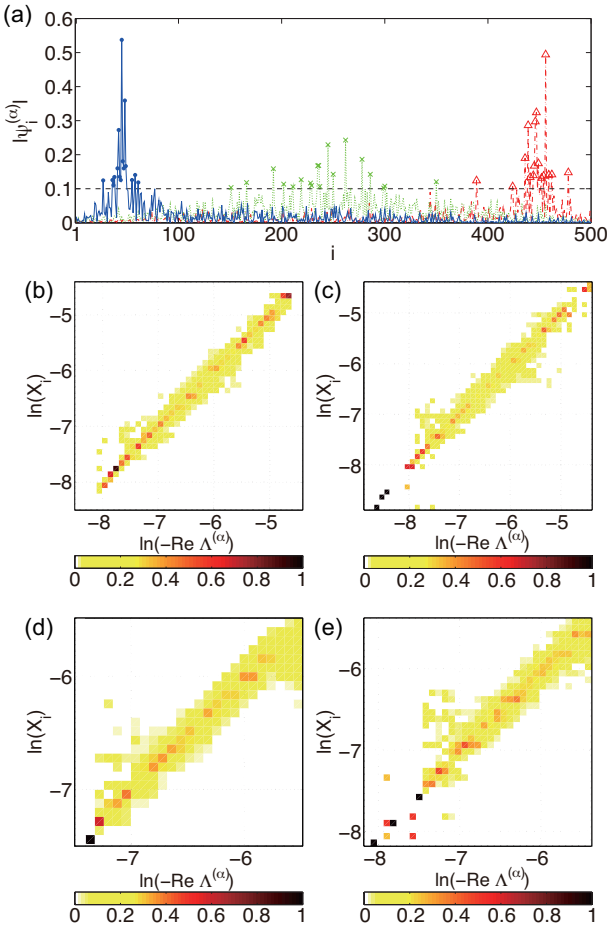

Figure 1: Localization of advection eigenvectors. (a) Three advection eigenvectors for $\alpha = 50$ (blue solid curve), $\alpha = 250$ (green dotted curve), and $\alpha = 450$ (red chained curve) in a scale-free network. Magnitudes $|\psi_i^{(\alpha)}|$ are plotted and large-deviation nodes where $|\psi_i^{(\alpha)}| > 0.1$ are marked by dots ($\alpha = 50$), crosses ($\alpha = 250$), and triangles ($\alpha = 450$). (b-e) Density plot of the large-deviation points for (b,c) Barabási-Albert, and (d,e) Erdös-Rényi networks. Transportation capacity W_{ij} is either (b,d) equal for all links, i.e., $W_{ij} = 1$, or (c,e) randomly drawn from the uniform distribution $0 < W_{ij} < 1$. The network size and mean degree are fixed at $N = 500$ and $\langle k \rangle = 20$, respectively, for all networks. Counting intervals for these density maps are (b,c) $\Delta[\ln(-\mathrm{Re}\Lambda^{(\alpha)})] = \Delta[\ln(X_i)] = 0.1$ and (d,e) $\Delta[\ln(-\mathrm{Re}\Lambda^{(\alpha)})] = \Delta[\ln(X_i)] = 0.08$.

First, we show in Fig. 1 the localization of the advection eigenvectors. Note that the advection matrix is generally asymmetric, such that the eigenvector components may have complex values and these values are displayed

by using the magnitudes $\left|\psi_i^{(\alpha)}\right|$ of each component.

Three different eigenvectors of a scale-free network are displayed in Fig. 1 (a). This scale-free network was generated by the Barabási-Albert preferential attachment algorithm [6]. The transport capacities of all links are set to $W_{ij} = 1$. It can be seen in the figure that all three eigenvectors localize in the network. Moreover, the eigenvector with smaller α is localized on the subset of nodes with smaller i ($\alpha = 50$), whereas the eigenvector with larger α is localized at nodes with larger i ($\alpha = 450$). This indicates the correlation between the variable $\mathrm{Re}\Lambda^{(\alpha)}$ and the flow intensity X_i at the localized node because we sort indices α and i as Eqs. (5) and (8).

It is shown in Fig. 1 (b) that the localization holds for all eigenvectors. The density plot has been constructed as follows: All nodes were divided into groups according to their flow intensities X_i. Each group contained the nodes with X_i within the window of width 0.1 for $\ln(X_i)$. The variable $\ln(-\mathrm{Re}\Lambda^{(\alpha)})$ was also divided into equal intervals of window width 0.1. In each two-dimensional interval, the number of large-deviation nodes specified by $\left|\psi_i^{(\alpha)}\right| > 0.1$ are counted. The resulting relative number of large-deviation nodes in each interval is displayed as a density plot. As can be seen, a clear diagonal structure is observed in the plots, indicating that the characteristic flow intensity X_α exists for each eigenmode α specifying the localized subset and

$$-\mathrm{Re}\Lambda^{(\alpha)} \simeq X_\alpha, \tag{9}$$

holds. This localization property can be found even when the transportation capacity W_{ij} is not equal but rather randomly chosen [Fig. 1 (c)]. Furthermore, it is not sensitive to the network architecture [Fig. 1 (d) and (e) for Erdös-Rényi networks [7]].

3. Perturbation approximation of advection eigenvectors

3.1. Perturbation approximation

To explain the localization of the advection eigenvectors, we propose a perturbation approach. In the advection matrix, the diagonal elements represent the total passing flows on the nodes, $M_{ii} = -X_i$, whereas the non-diagonal elements are the incoming flow along the links, $M_{ij} = J_{ij}A_{ij}$ ($i \neq j$). The total flow X_i is divided at each node into flows J_{ji} along the outgoing links, resulting in non-diagonal elements of the order $O(\langle X\rangle/\langle k\rangle)$, where $\langle k\rangle = \sum_{i,j=1}^N W_{ij}A_{ij}/N$ is the mean degree of the network.

Thus, by introducing a parameter $\epsilon = \langle k\rangle^{-1}$, the advection matrix can be split as

$$\mathbf{M} = \mathbf{M}_0 + \epsilon\mathbf{M}_1, \tag{10}$$

so that matrix elements $M_{0,ij} = -X_i\delta_{i,j}$ and $M_{1,ij} = \langle k\rangle J_{ij}A_{ij}$ have the same order $O(\langle X\rangle)$. If the network is sufficiently dense, $\epsilon = \langle k\rangle^{-1} \ll 1$ holds. Thus, we can apply the perturbation approximation to evaluate eigenvectors. A similar perturbation approach was used to analyze the eigenvalues of the Laplacian matrix [8].

It is convenient to employ the bra-ket notation to denote the advection eigenvectors, $\vec{\psi}^{(\alpha)} = |\alpha\rangle$, and drop the summation symbol as $\sum_{j=1}^N M_{ij}\psi_j^{(\alpha)} = M|\alpha\rangle$. We expand the advection eigenvectors and eigenvalues in the series of the parameter ϵ as

$$|\alpha\rangle = |\alpha\rangle_0 + \epsilon|\alpha\rangle_1 + \epsilon^2|\alpha\rangle_2 + \cdots, \tag{11}$$
$$\Lambda^{(\alpha)} = \Lambda_0^{(\alpha)} + \epsilon\Lambda_1^{(\alpha)} + \epsilon^2\Lambda_2^{(\alpha)} + \cdots, \tag{12}$$

and substitute them into the eigenvalue equation $M|\alpha\rangle = \Lambda^{(\alpha)}|\alpha\rangle$ to obtain a set of perturbation equations. In the present study we use the equations up to the second order of ϵ:

$$\left(L_0 - \Lambda_0^{(\alpha)}\right)|\alpha\rangle_0 = 0, \tag{13}$$
$$\left(L_0 - \Lambda_0^{(\alpha)}\right)|\alpha\rangle_1 = -\left(L_1 - \Lambda_1^{(\alpha)}\right)|\alpha\rangle_0, \tag{14}$$
$$\left(L_0 - \Lambda_0^{(\alpha)}\right)|\alpha\rangle_2 = -\left(L_1 - \Lambda_1^{(\alpha)}\right)|\alpha\rangle_1 + \Lambda_2^{(\alpha)}|\alpha\rangle_0. \tag{15}$$

The exact solution of the zeroth-order equation (13) can be found as

$$|\alpha\rangle_0 = (0, \cdots, 0, \overset{\alpha}{\overset{\vee}{1}}, 0, \cdots, 0)^{\mathrm{t}} \quad \text{and} \quad \Lambda_0^{(\alpha)} = -X_\alpha, \tag{16}$$

for $\alpha = 1, ..., N$. Each eigenvector has a single non-vanishing element at the network node $i = \alpha$, and the corresponding eigenvalue $\Lambda_0^{(\alpha)}$ is equal to the negative of the total passing flow X_α at that node. Note that the zeroth-order approximation (16) can explain the relation between the spectrum and the characteristic flow intensity, i.e., Eq. (9).

By examining the perturbation equations (13)-(15), we calculate the higher-order corrections to the eigenvector up to the second order; $|\alpha\rangle_{\mathrm{approx}} = |\alpha\rangle_0 + \epsilon|\alpha\rangle_1 + \epsilon^2|\alpha\rangle_2$. If there is a degeneration, i.e., a set of zeroth-order eigenvectors belongs to the same eigenvalue, we should employ the *degenerate* perturbation theory to calculate perturbation corrections. In the present case, we numerically verified that no degeneration exists in all the networks considered in Fig. 1. Thus, here we use the standard perturbation theory.

The first- and second-order correction can be obtained as follows (see e.g., [5] for the derivation):

$$|\alpha\rangle_1 = \sum_{\beta\neq\alpha} |\beta\rangle_0 \frac{{}_0\langle\beta|M_1|\alpha\rangle_0}{\Lambda_0^{(\alpha)} - \Lambda_0^{(\beta)}}, \tag{17}$$
$$|\alpha\rangle_2 = \sum_{\beta\neq\alpha}\sum_{\gamma\neq\alpha} |\beta\rangle_0 \frac{{}_0\langle\beta|M_1|\gamma\rangle_0\,{}_0\langle\gamma|M_1|\alpha\rangle_0}{(\Lambda_0^{(\alpha)} - \Lambda_0^{(\beta)})(\Lambda_0^{(\alpha)} - \Lambda_0^{(\gamma)})} - \sum_{\beta\neq\alpha} |\beta\rangle_0 \frac{{}_0\langle\beta|M_1|\alpha\rangle_0\,{}_0\langle\alpha|M_1|\alpha\rangle_0}{(\Lambda_0^{(\alpha)} - \Lambda_0^{(\beta)})^2}. \tag{18}$$

The second term on the right hand side of Eq. (18) vanishes in the present case because ${}_0\langle\alpha|M_1|\alpha\rangle_0 = \langle k\rangle J_{ii}A_{ii} = 0$.

3.2. Predicted advection eigenvectors

In Figure 2, the predicted eigenvectors are displayed in the density plots as used in Fig. 1. It can be seen in the figures that, in the predicted eigenvectors, the large-deviation nodes exhibit diagonal structures for all considered networks. This indicates that the perturbation approximation can explain the localization of the advection eigenvectors.

Moreover, it can also explain the localization strength of each eigenvector. As can be seen in Fig. 1 (a), eigenvectors with either a large or small class of α strongly localize in the network, i.e., large-deviation points are shared by a small number of nodes ($\alpha = 50$ and 450). By contrast, the localization of eigenvectors with an intermediate class of α is weak and, a relatively large number of nodes share the large-deviation points ($\alpha = 250$). These characteristics are represented by the color map of the density plot. Strongly localized nodes are represented by a dark color because the number of nodes sharing large-deviation points is small, which causes the density to become high at these nodes. It can be seen in Fig. 2 that the color code in the density plot is qualitatively reproduced in the results of the perturbation approximation, thereby indicating the ability of the approximation to predict the localization pattern of the advection eigenvectors.

Note that Eqs. (17) and (18) indicate that each component of the approximate eigenvectors has real values whereas, as mentioned before, the advection eigenvectors may generally have components consisting of complex values. Thus, the perturbation approach cannot predict the eigenvectors quantitatively. Nevertheless, it is remarkable that the localization properties are successfully reproduced.

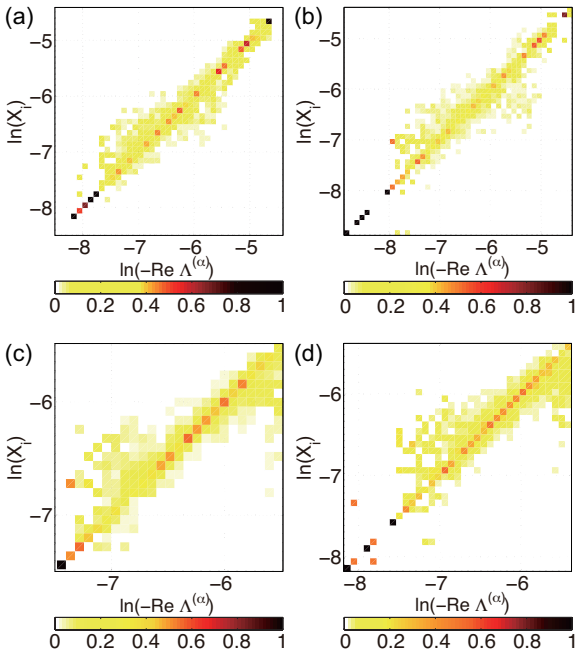

Figure 2: Prediction of the advection eigenvectors used in Fig. 1. Density plot of the large-deviation points for (a,b) Barabási-Albert, and (c,d) Erdös-Rényi networks. Transportation capacity W_{ij} is either (a,c) equal for all links, i.e., $W_{ij} = 1$, or (b,d) randomly drawn from the uniform distribution $0 < W_{ij} < 1$. Counting intervals for these density maps are (a,b) $\Delta[\ln(-\mathrm{Re}\Lambda^{(\alpha)})] = \Delta[\ln(X_i)] = 0.1$ and (c,d) $\Delta[\ln(-\mathrm{Re}\Lambda^{(\alpha)})] = \Delta[\ln(X_i)] = 0.08$.

4. Conclusions

In this work, we developed a perturbation approach to explain the localization of the advection eigenvectors in networks. We divided the advection matrix into two parts corresponding to the diagonal and non-diagonal elements. If the network is sufficiently dense, the components of these two matrices have a distinct order, so that we could use the perturbation approximation to evaluate the eigenvectors and eigenvalues. We calculated the perturbation corrections up to the second order.

It was found that the zeroth-order approximation can explain the correlation between the real parts of the advection eigenvalues and the characteristic flow intensities of localized nodes. Moreover, the second-order approximation can reproduce the localization property of the advection eigenvectors. The results are neither sensitive to the network architecture nor to the weight of links.

Acknowledgments

Financial support through JSPS KAKENHI Grant Number 15K12111 in Japan is gratefully acknowledged.

References

[1] F. Pasquill and F. B. Smith, *Atmospheric Diffusion* (Ellis Horwood, Chichester, 1983).

[2] A. Mafraneto and R. T. Carde, "Fine-scale structure of pheromone plumes modulates upwind orientation fo flying moths", *Nature* **369**, 142 (1994).

[3] B. L. Shraiman and E. D. Siggla, "Scalar turbulence", *Nature* **405**, 639 (2000).

[4] S. Hata, H. Nakao and A. S. Mikhailov, "Advection of passive particles over flow networks", *Phys. Rev. E* **89**, 020802(R) (2014).

[5] J. J. Sakurai and J. J. Napolitano, *Modern Quantum Mechanics* (Pearson Education Ltd., London, 2013).

[6] A.-L. Barabási and R. Albert, "Emergence of scaling in random networks", *Science* **286**, 509 (1999).

[7] P. Erdös and A. Rényi, "On random graphs. I", *Publicationes Mathematicae* **6**, 290 (1959).

[8] D.-H. Kim and A. E. Motter, "Ensemble averageability in network spectra", *Phys. Rev. Lett.* **98**, 248701 (2007).